Eurasian Journal of Physics and Functional Materials

2024, 8(1), 14-22

Determination of phase boundaries and diffusion coefficients of copper in spinel $CuCr_2Se_4$ and delafossite $CuCrSe_2$ by galvanostatic intermittent titration technique (GITT)

A.O. Onishenko, E.A. Suslov, M.S. Postnikov, A.S. Shkvarin, A.N. Titov, A.I. Merentsov*

M.N. Mikheev Institute of Metal Physics of Ural Branch of Russian Academy of Sciences, Yekaterinburg, Russia

E-mail: alexander.merentsov@urfu.ru

DOI: **10.32523/ejpfm.2024080102**
Received: 23.01.2024 - after revision

Cu_xCrSe_2 materials can exist in the form of delafossite with a layered structure and exhibit multiferroic properties, or in the form of spinel and exhibit ferromagnetic properties, depending on the copper concentration. The stability of both forms of Cu_xCrSe_2 has been studied with regards to defectivity in the copper sublattice. The boundaries of the Cu_xCrSe_2 homogeneity regions for the delafossite-like structure and for the cubic spinel $CuCr_2Se_4$ were determined by coulometric titration at room temperature. Analysis of the time dependence of cell polarization allowed us to estimate the diffusion coefficients in these materials.

Keywords: delafossite; layered structure; multiferroic properties; cubic spinel; ferromagnetic properties

Introduction

Multiferroic magnetoelectric materials exhibit ferroelectric and ferromagnetic properties, providing technological prospects in new multifunctional devices

[1–3]. For example, multiferroics are used in memory devices [4]. It is known [5, 6], that various alloys with magnetic properties are widely used in various microdevices, however layered dichalcogenides like $CuCrSe_2$ also exhibit interesting magnetic properties and memory elements can be developed based on such materials [1–3]. In layered materials like $CuCrSe_2$ with R3m structure, Cu atoms are distributed only in one tetrahedral plane [7]. As a result, the crystal lattice is non-centrosymmetric, allowing for electric polarization of the crystal along the c axis [1]. The temperature of spontaneous polarization coincides with the temperature of magnetic ordering in the Cr sublattice. It is known [8] that the main interaction in the Cr sublattice is ferromagnetic. However, the regular triangular sublattice prohibits ferromagnetic ordering and leads to frustrations. It seems that frustrations are highly dependent on the level of defectivity in the Cu sublattice. This is because the asymmetric environment in the chromium sublattice causes the material to be multiferroic. Therefore, it is crucial to investigate the level of defectiveness in this material. Studying defectiveness in spinel is significant as it helps to understand the impact of the lattice structure on the permissible level of defectiveness.

$CuCrSe_2$ has a crystal structure [9] similar to that of delafossite ($CuCrO_2$) [10], which is shown in Figure 1a. The compound $CuCr_2Se_4$ (or $Cu_{0.5}CrSe_2$) is known for its spinel structure [11] (Figure 1b). The delafossite lattice of $CuCrSe_2$ can be described as a lattice of $CrSe_2$ layers intercalated with copper. While there is literature available on spinel $CuCr_2Se_4$, there is a need for data on phase diagrams in the Cu_xCrSe_2 system needs to be present [12]. The similarity with intercalation compounds suggests a possible region of homogeneity for both $CuCrSe_2$ and $Cu_{0.5}CrSe_2$.

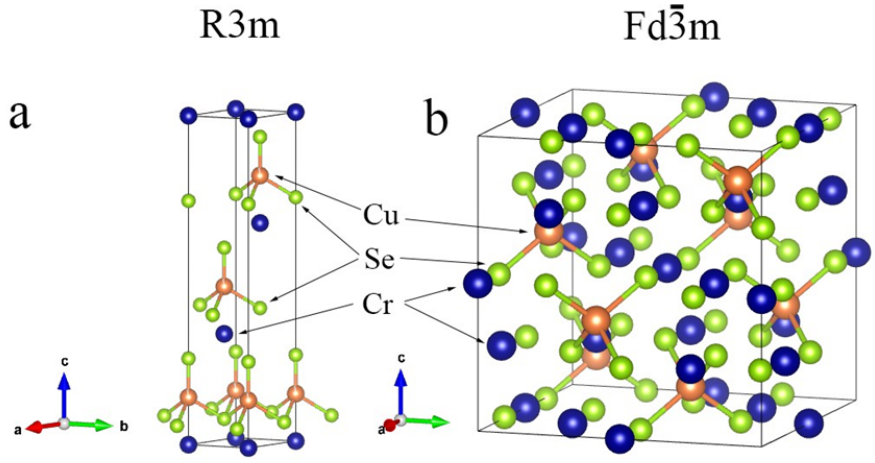

Figure 1. Unit cells of $CuCrSe_2$ (a) and $CuCr_2Se_4$ (b).

The density of Cr 3d states in $CrSe_2$ was theoretically predicted to be half-metallic with 100% spin polarization [13]. The possibility of obtaining $CrSe_2$ from K_xCrSe_2 was demonstrate in [14, 15] according to the following reaction:

$$2KCrSe_2 + I_2 \rightarrow 2KI + 2CrSe_2, \quad (1)$$

$CrSe_2$ layered and spinel structures can be obtained using this approach.

$CrSe_2$ material should be obtained without heating since it is unstable and decomposes at a temperature of 600 K according to reaction (2) [15]:

$$2CrSe_2 \rightarrow Cr_2Se_3 + Se, \tag{2}$$

The aim of this study was to investigate phase equilibria in the $CrSe_2$ – Cu_xCrSe_2 (delafossite) and $CrSe_2$ – $Cu_xCr_2Se_4$ (spinel) systems at room temperature.

Methods

Samples of Cu_xCrSe_2 and $Cu_xCr_2Se_4$ were synthesized using precise weighed amounts (0.0001 g) of elements in evacuated quartz ampoules via the solid-phase method. This approach ensures purer products free of chloride impurities during syntheses from solutions [16]. The synthesis was carried out in several stages with repeated homogenization. Based on the experience of the authors [14, 15], $CrSe_2$ from $CuCrSe_2$ was obtained using a similar method through the following reactions:

1^{st} stage

$$Cu + 2Cr + 4Se \rightarrow CuCr_2Se_4(\text{space group } Fd\,\bar{3}\,m), \tag{3}$$

$$Cu + Cr + 2Se \rightarrow CuCrSe_42(\text{space group R3m}), \tag{4}$$

2^{nd} stage

$$2CuCrSe_2 + I_2 \rightarrow 2CuI + 2CrSe_2(\text{space group R3m}), \tag{5}$$

$$4CuCrSe_2 + I_2 \rightarrow 2CuI + 4Cu_2CrSe_2(\text{space group R3m}), \tag{6}$$

$$2CuCr_2Se_4 + I_2 \rightarrow 2CuI + 2Cr_2Se_4(\text{space group } Fd\,\bar{3}\,m), \tag{7}$$

Single-phase finely dispersed $CuCrSe_2$ and $CuCr_2Se_4$ powders, crystalline iodine I_2, and acetonitrile CH3CN were used for synthesis. Prior to synthesis, residual water was removed from acetonitrile using molecular sieves (4A NaA). A stoichiometric amount of compounds and iodine was taken and 10 wt. % excess of iodine was added. Being the synthesis medium, acetonitrile was taken in excess. The synthesis was carried out for one week with periodic stirring of the samples in an ultrasonic bath once a day for 30 minutes. After 7 days, the resulting products were filtered and washed with acetonitrile to remove CuI, then dried to remove acetonitrile vapor.

The homogeneity of the synthesized samples was checked using X-ray powder diffraction (XRD) on a Shimadzu XRD 7000 Maxima diffractometer (monochromatic CuKα radiation, λ =1.5406 Å, scanning 2θ angle range of 10°–90°, Bragg-Brentano geometry) in the Collective Use Center "Ural-M" of the Institute of Metallurgy, Russian Academy of Sciences, Ural Division.

Copper was removed from $CuCrSe_2$ and $CuCr_2Se_4$ electrochemically using the galvanostatic intermittent titration method (GITT) for coulometric titration. The electrochemical cells used were $Cu|Cu^+|Cu_xCrSe_2$ and $Cu|Cu^+|Cu_xCr_2Se_4$ for the Cu_xCrSe_2 and $Cu_xCr_2Se_4$ systems, respectively. Metallic copper was used as the counter and negative electrode. The cathode material consisted of $Cu_xCr_ySe_2$:C45 Carbon Black:Polyvinylidene fluoride at 80:10:10 wt.%, respectively. A 0.1M solution of CuI in acetonitrile was used as an electrolyte. The search for phase boundaries was conducted through coulometric titration with a titration step of dx=0.025 mol (2.5 mol%). Electrochemical measurements were conducted at room temperature using a BTS-4000 (5V, 10mA) potentiostat. The principles of determining phase boundaries through the electromotive force (EMF) method and the GITT method are described in [17–20].

Results and discussion

The results of coulometric titration are presented in Figure 2.

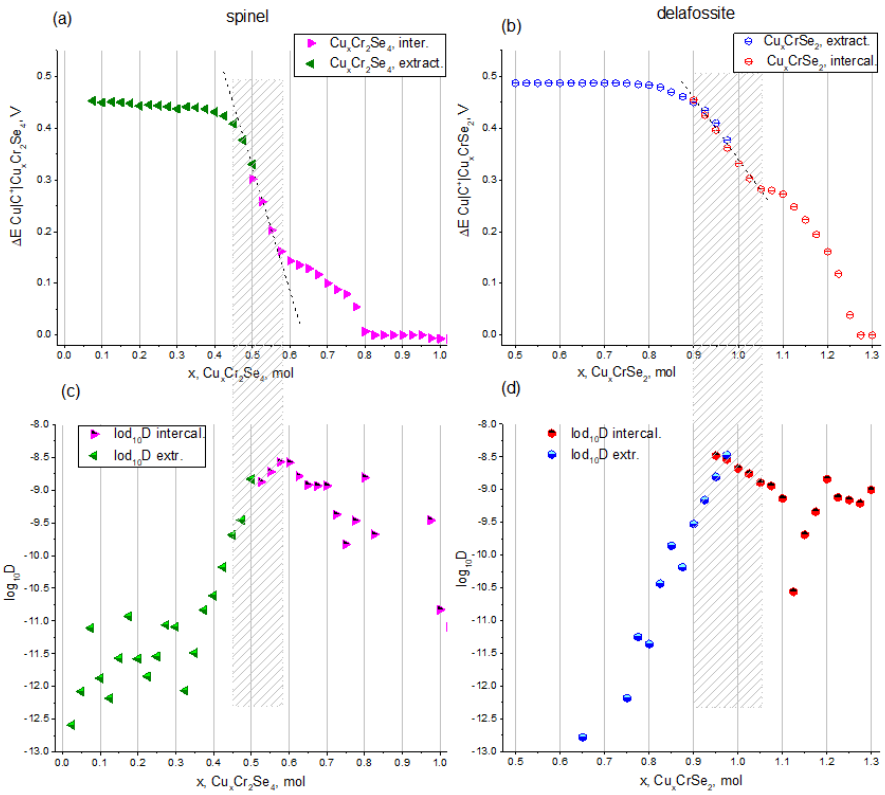

Figure 2. Dependencies of coulometric titration $\Delta E \sim f(x)$ in electrochemical cells $Cu|Cu^+|CuxCrSe_2$ (a) and $Cu|Cu^+|CuxCr_2Se_4$ (b); dependence of the logarithm of the diffusion coefficient (log10D) on the Cu content in spinel $CuCr_2Se_4$ (c) and delafossite $CuCrSe_2$ (d).

Figure 2 shows a large homogeneity region of approximately 15 mol.% and wide two-phase regions for both Cu_xCrSe_2 (spinel and delafossite) systems. Homogeneity regions were found to be in the Cu concentration range of 0.9<x<1.2 (0.45 <x<0.6 in terms of $Cu_{0.5}CrSe_2$) for spinel $Cu_xCr_2Se_4$ and of 0.9<x<1.05 for delafossite Cu_xCrSe_2 . The Cu concentration range of x>0.8 for $Cu_xCr_2Se_4$ corresponds to the precipitation of Cu or to the formation of Cu dendrites in the

electrochemical cell. A similar region exists at x>1.27 for the Cu_xCrSe_2 system. The ranges of x<0.45 and of 0.6<x<0.8 correspond to two-phase regions for $Cu_xCr_2Se_4$. Similarly, the ranges of x<0.9 and of 1.05<x<1.1 correspond to two-phase regions for Cu_xCrSe_2. The range of 1.1<x<1.27 is presumed to correspond to a two or three-phase region, possibly including $Cu_{1+\sigma}CrSe_2$, $Cu_{1.75-1.82}Se$, and Cu.

The experimental data analysis enabled us to determine the diffusion coefficient order. In this case, we used the technique described in [21–23], which involves analyzing the dependence of $\Delta E \sim f(t)$ after turning the titration current on and off and solving equation (8):

$$D = \frac{4}{\pi t} L^2 (\frac{\Delta E_S}{\Delta E_t})^2 t << L^2/D, \quad (8)$$

where t is the duration of the current pulse; L – diffusion length (electrode thickness); ΔE_s – potential difference when the current is turned off; ΔE_t is the potential difference when passing current excluding iR.

Figure 2c and Figure 2d show the Cu concentration dependences of the diffusion coefficients for $CuCr_2Se_4$ and $CuCrSe_2$, respectively. The maximum diffusion mobility for $CuCr_2Se_4$ (D=$10^{-8.5}$ cm^2/s) and $CuCrSe_2$ (D=$10^{-8.5}$ cm^2/s) corresponds to the stoichiometric compositions. Deviation from stoichiometry may result in a deficiency of mobile Cu ions or vacancies available for filling.

The diffusion coefficients decrease when defects occur with increasing and decreasing Cu content, as in the case of $CuCr_2Se_4$ spinel. The diffusion coefficient reaches a minimum value at x=0.3 and remains almost constant with a further decrease in Cu content (Figure 2c). This Cu concentration is in good agreement with the percolation threshold for a cubic lattice (0.31 for the problem of cubic lattice nodes with interaction between nearest neighbors [24]). Forming of $Cu_{1.75-1.82}Se$ is possible when moving towards compositions with high Cu content. The decrease of D at x>0.7 may be associated with the work to destroy the structure.

Figure 2d shows the dependence of the diffusion coefficient on the Cu content for the $CuCrSe_2$ system. The maximum value of D corresponds to the composition $Cu_{0.95}CrSe_2$. Increasing or decreasing the Cu content results in a decrease in D values, which may be attributed to the hindered movement of Cu ions due to defects along its sublattice.

It is worth noting that the boundary of the region with a sharp increase in the scatter of the Cu diffusion coefficient in $CuCr_2Se_4$ (0<x<0.3 in Figure 2c) coincides with the boundary of the single-phase region according to electrochemical data. This may be due to the material's inhomogeneity ($CrSe_2$), which complicates the diffusion process. However, in the case of $CuCrSe_2$, such an increase in scatter when crossing the boundary of the single-phase region is not observed (Figure 2d). The difference between copper's role in the lattice of layered $CrSe_2$ and spinel $CuCr_2Se_4$ is evident. In the former, copper acts as an intercalated impurity, while in the latter, it is an essential part of the crystal structure. In the regions corresponding to cubic $CrSe_2$, copper's mobility is negligible.

To determine the chemical composition of the samples obtained by chemical extraction of Cu, an energy-dispersive X-ray (EDX) analysis was used. The averaging of the chemical composition was conducted over at least 10 points. Scanning electronic microscope (SEM) images were obtained on a Quanta-200 microscope. Figure 3 shows SEM images of $CrSe_2$, $Cu_{0.5}CrSe_2$ and $CuCr_2Se_4$ at the same magnification.

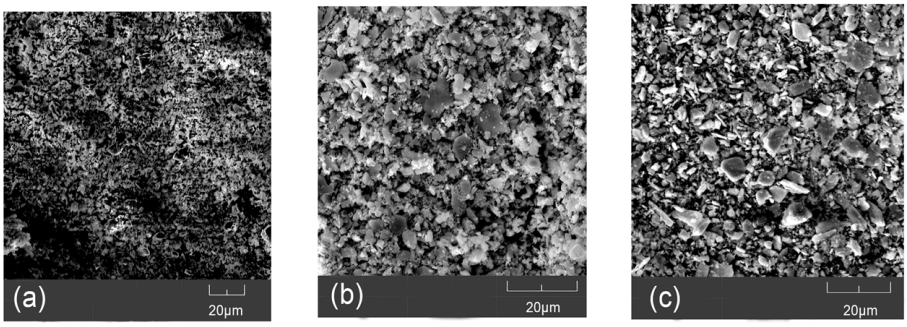

Figure 3. SEM images of $CrSe_2$ (a), $Cu_{0.5}CrSe_2$ (b) and $CuCr_2Se_4$ (c) after chemical extraction of copper.

SEM images of $CrSe_2$, $Cu_{0.5}CrSe_2$, and $CuCr_2Se_4$ were processed using the ImageJ software package [25]. The resulting distribution of the number of grains by their area is shown in Figure 4.

The chemical compositions of the obtained samples are listed in Table 1.

Table 1.
Chemical composition of Cu_xCrSe_2 compounds before and after copper extraction.

Initial compound	Expected compound	Chemical composition of the obtained samples
$CuCrSe_2$	$CrSe_2$	$Cu_{0.24}CrSe_2$
$CuCrSe_2$	$Cu_{0.5}CrSe_2$	$Cu_{0.568}CrSe_2$
$CuCrSe_2$	$CrSe_2$	$Cu_{0.76}Cr_2Se_{3.74}$

The initial $CuCr_2Se_4$ crystal structure is described by cubic ordering $Fd\bar{3}m$ with a lattice parameter of a=10.326 Å, which agrees with the literature data [12].

The diffraction pattern's general profile remained unchanged after copper was chemically extracted from $CuCr_2Se_4$. An additional low-intensity peak at 46 degrees, corresponding to elemental copper, appeared. This peak was most likely formed during the decomposition of the CuI reaction product. The lattice parameter of a=10.323 Åremains unchanged within the calculation error. Table 2 presents the results of a full-profile analysis of the diffraction patterns performed using the GSAS II software package [26]. A copper defectivity of 6% in the $CuCr_2Se_4$ phase is observed.

A full-profile analysis of an XRD pattern of $CrSe_2$ obtained from $CuCrSe_2$ (Figure 5) shows that even after chemical extraction of Cu, it remains within the lattice to some extent. This may be due to the presence of both large and small particles in the starting substance powder, as shown in Figure 3, which causes non-uniform reaction. A lattice copper concentration according to full-profile analysis is of x=0.24, which is consistent with the EDX findings presented in Table 1.

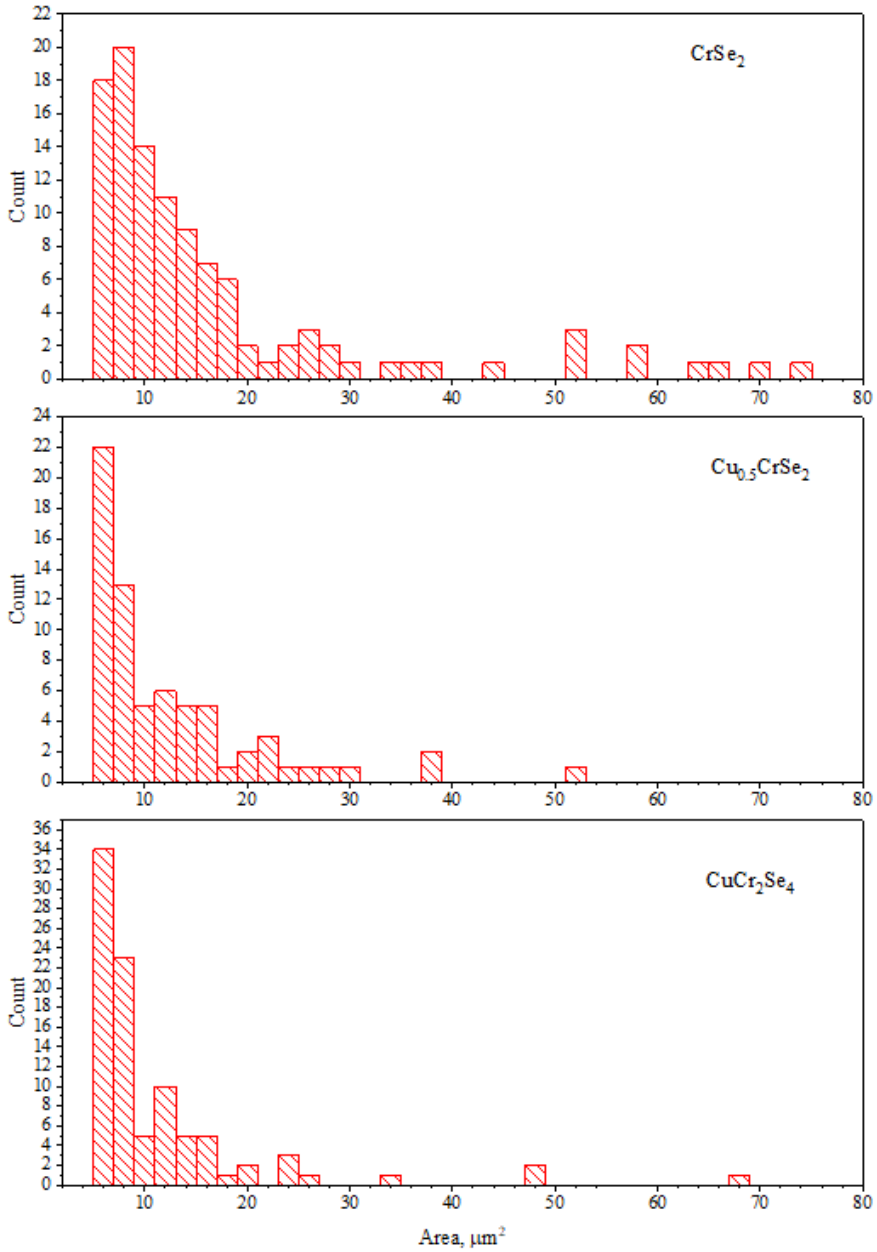

Figure 4. Distribution of the number of grains by their area for $CrSe_2$, $Cu_{0.5}CrSe_2$ and $CuCr_2Se_4$.

Table 2.
Full-profile refinement results for $CuCr_2Se_4$.

Compound	Unit cell	Atom	Coordinates	Filling	Convergence Options
$CuCr_2Se_4$	$Fd\bar{3}m$	Cu	0.125 0.125 0.125	1	Rf^2=9.17%
	a=10.326Å	Cr	0.5 0.5 0.5	1	wRp=13.65%
		Se	0.257 0.257 0.257	1.0494	χ^2=4.356
$CuCr_2Se_4$	$Fd\bar{3}m$	Cu	0.125 0.125 0.125	0.9405	Rf^2=11.14%
after Cu	a=10.323Å	Cr	0.5 0.5 0.5	1	wRp = 11.79%
extraction		Se	0.257 0.257 0.257	1	χ^2=4.337

It is worth noting that for isostructural $CuCrS_2$, a single-phase material with a composition of approximately $Cu_{0.66}CrS_2$ was obtained through the chemical

extraction of copper [14]. This composition coincides with the composition of spinel – $CuCr_2S_4$; however, it retains a layered structure with trigonal symmetry. The EMF of the electrochemical cell's "plateau" region indicates that it is composed solely of a mixture of $CrSe_2$ and $CuCrSe_2$. This suggests that there is no layered compound with the composition of $Cu_{0.5}CrSe_2$ present in this system.

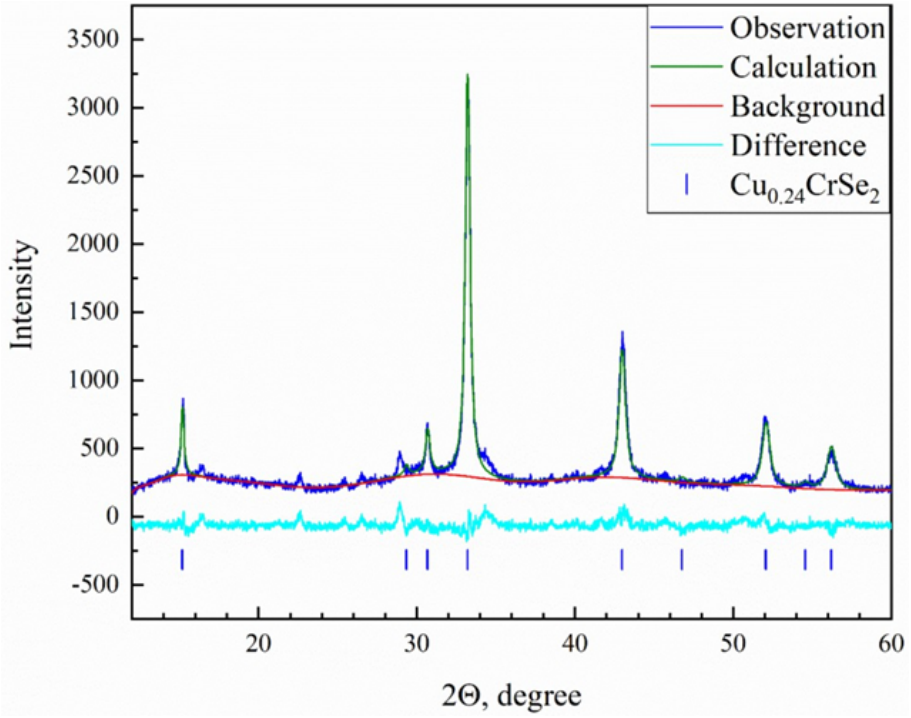

Figure 5. XRD pattern of $Cu_{0.24}CrSe_2$ after chemical copper extraction.

It can be assumed that the defectiveness of the resulting sample is associated with a blocking effect. This means that copper is extracted from the surface of crystals [27].

Conclusions

The current study has established for the first time the copper homogeneity regions for $CuCrSe_2$ with a delafossite structure and $CuCr_2Se_4$ with a spinel structure and assessed their width. In thermodynamic analysis of phase relationships, it is important to consider the presence of noticeable regions of homogeneity in these materials.

Chemical and electrochemical methods were used to partially extract copper from the $CuCrSe_2$ and $CuCr_2Se_4$ compounds. It was found that chemical extraction is gentler and does not damage the matrix. The maximum value of diffusion coefficients $D = 10^{-8.5}$ cm^2/s was achieved at compositions close to stoichiometric for both $CuCrSe_2$ and $CuCr_2Se_4$ systems. An increase in the number of defects results in a decrease in the values of diffusion coefficients.

Acknowledgements

Funding for this research was provided by: Russian Science Foundation (project No. 22-13-00361).

References

[1] M. Fiebig et al., Nat. Rev. Mater. **1** (2016) 16046. [*CrossRef*]
[2] T. Zhong et al., Natl. Sci. Rev. **7** (2020) 373–380. [*CrossRef*]
[3] S.N. Achary et al., Functional Materials (2012) 155–191. [*CrossRef*]
[4] K. Roy et al., Nat. Nanotechnol. **8** (2013) 826–830. [*CrossRef*]
[5] V. Fedkin et al., Ceram. Int. **49** (2023) 28089–28097. [*CrossRef*]
[6] A. Kotelnikova et al., RSC Adv. **12** (2022) 35722–35729. [*CrossRef*]
[7] A. Gagor, D. Gnida, A. Pietraszko, Mater. Chem. Phys. **146** (2014) 283–288. [*CrossRef*]
[8] G.C. Tewari et al., Mater. Chem. Phys. **145** (2014) 156–161. [*CrossRef*]
[9] R. Yano, T. Sasagawa, Cryst. Growth Des. **16** (2016) 5618–5623. [*CrossRef*]
[10] J.-P. Doumerc et al., Mater. Res. Bull. **21** (1986) 745–752. [*CrossRef*]
[11] I. Okonska-Kozlowska et al., Acta Cryst. C **49** (1993) 1448–1449. [*CrossRef*]
[12] H. Lu et al., Crystals **12** (2022) 433. [*CrossRef*]
[13] C.M. Fang et al., J. Phys. Condens. Matter. **9** (1997) 10173–10184. [*CrossRef*]
[14] A.-L. Hansen et al., J. Mater. Chem. C. **5** (2017) 9331–9338. [*CrossRef*]
[15] C.F. van Bruggen et al., Phys. B+C. **99** (1980) 166–172. [*CrossRef*]
[16] X. Song et al., Chem. Mater. **33** (2021) 8070–8078. [*CrossRef*]
[17] J. Molenda, Solid State Ionics **176** (2005) 1687–1694. [*CrossRef*]
[18] E.A. Suslov et al., J. Phys. Chem. A. **125** (2021) 1981–1986. [*CrossRef*]
[19] M. Matlak et al., Phys. Rev. B. **63** (2001) 052101. [*CrossRef*]
[20] M.S. Postnikov et al., Mater. Lett. **353** (2023) 135222. [*CrossRef*]
[21] W. Weppner and R.A. Huggins, J. Electrochem. Soc. **124** (1977) 1569–1578. [*CrossRef*]
[22] Y. Zhu, C. Wang, J. Phys. Chem. C. **114** (2010) 2830–2841. [*CrossRef*]
[23] Z. Shen et al., J. Electrochem. Soc. **160** (2013) A1842–A1846. [*CrossRef*]
[24] I.M. Sokolov, Sov. Phys. Uspekhi. **29** (1986) 924–945. [*CrossRef*]
[25] C.A. Schneider et al., Nat. Methods **9** (2012) 671–675. [*CrossRef*]
[26] B.H. Toby, R.B. Von Dreele, J. Appl. Cryst. **46** (2013) 544–549. [*CrossRef*]
[27] E.A. Suslov et al., Ionics **22** (2016) 503–514. [*CrossRef*]